ACS APPLIED MATERIALS & INTERFACES

Research Article

www.acsami.org

Cationic Conjugated Polymer/Hyaluronan-Doxorubicin Complex for Sensitive Fluorescence Detection of Hyaluronidase and Tumor-Targeting Drug Delivery and Imaging

Yanqin Huang,*[,†] Caixia Song,[†] Huichang Li,[†] Rui Zhang,*[,§] Rongcui Jiang,[†] Xingfen Liu,[†] Guangwei Zhang,[†] Quli Fan,[†] Lianhui Wang,[†] and Wei Huang*[,†,‡]

[†]Key Laboratory for Organic Electronics & Information Displays (KLOEID) and Institute of Advanced Materials (IAM), Jiangsu National Synergetic Innovation Center for Advanced Materials (SICAM), Nanjing University of Posts & Telecommunications, Nanjing 210023, China

[‡]Key Laboratory of Flexible Electronics (KLOFE) & Institute of Advanced Materials (IAM), Jiangsu National Synergetic Innovation Center for Advanced Materials (SICAM), Nanjing Tech University (NanjingTech), 30 South Puzhu Road, Nanjing 211816, China

[§]Department of Ophthalmology, Zhongda Hospital, Southeast University, Nanjing 211189, China

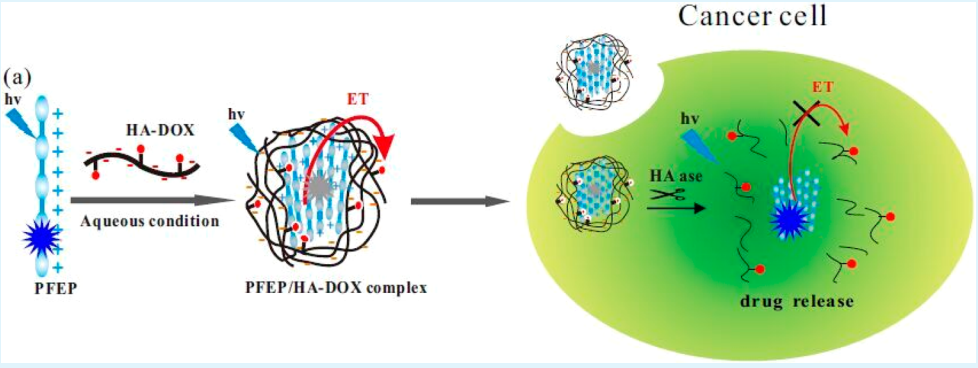

ABSTRACT: Hyaluronidase (HAase) is becoming a new type of tumor marker since it has been demonstrated to be overexpressed in various kinds of cancer cells. In this study, we described a novel fluorescence method for sensitive, rapid, and convenient HAase detection and tumor-targeting drug delivery and imaging, using a probe prepared by electrostatic assembly of a cationic conjugated polymer (CCP) and anionic hyaluronan (HA) conjugated with the anticancer drug doxorubicin (Dox). The CCP we used was poly{[9,9-bis(6′-(*N*,*N*,*N*-diethylmethylammonium)hexyl)-2,7-fluorenylene ethynylene]-*alt*-*co*-[2,5-bis(3′-(*N*,*N*,*N*-diethylmethylammonium)-1′-oxapropyl)-1,4-phenylene]} tetraiodide (PFEP). HA is a natural mucopolysaccharide that can be hydrolyzed by HAase into fragments with low molecular weights. In the PFEP/HA-Dox complex, the fluorescence of PFEP was efficiently quenched due to electron transfer from PFEP to Dox. After the PFEP/HA-Dox complex was exposed to HAase or was taken up by cancer cells through the specific binding between HA and CD44 receptor, HA was degraded by HAase to release the Dox, leading to the recovery of PFEP fluorescence to the "turn-on" state. Moreover, the degree of fluorescence recovery was quantitatively correlated with the concentrations of HAase. Compared with many previously reported methods, our work did not require laborious multiple modifications of HA that may affect the activity of HAase. This point, combined with the excellent optoelectronic property of conjugated polymer, endowed this method with high sensitivity (detection limit: 0.075 U/mL), high specificity, and rapid response, making it applicable for reliable and routine detection of HAase. This fluorescent probe was successfully utilized to detect HAase levels in human urine samples; furthermore, it can also be employed as a multifunctional system by realizing tumor-targeting drug delivery and cell imaging simultaneously. The development of this fluorescence method showed promising potential for early tumor diagnosis and therapy based on HAase detection.

KEYWORDS: *conjugated polymer, hyaluronan-doxorubicin, hyaluronidase, fluorescence, imaging*

INTRODUCTION

Hyaluronan (hyaluronic acid, HA), a negatively charged linear mucopolysaccharide, consists of repeating disaccharide units of β-(1,4)-D-glucuronic acid and β-(1,3)-*N*-acetyl-D-glucosamine.[1−3] It is abundant in extracellular matrixes and synovial fluids of all vertebrates and involved in many important biological processes, including tissue hydration, cell motility, proliferation and differentiation. Importantly, HA exhibits a high specific affinity for CD44 receptors overexpressed in many cancer cells and can enter cells through the receptor mediated

Received: July 26, 2015
Accepted: September 2, 2015
Published: September 2, 2015

DOI: 10.1021/acsami.5b06799
ACS Appl. Mater. Interfaces 2015, 7, 21529−21537

Scheme 1. (a) Schematic Illustration of the Overall Strategy for HAase Detection. (b) Chemical Structures of HA-Dox and PFEP

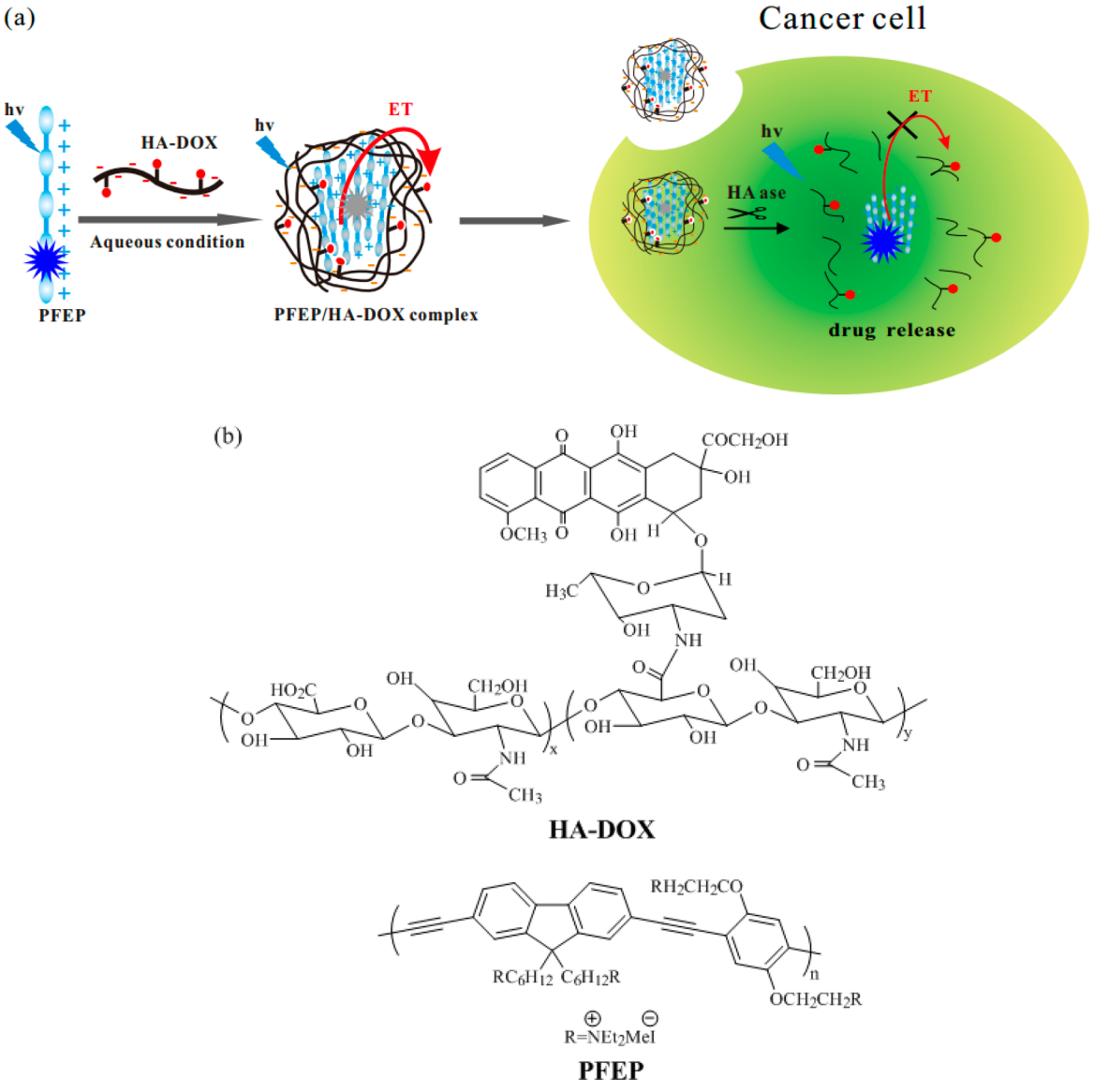

endocytosis;[1−5] moreover, its main chain can be hydrolyzed by hyaluronidase (HAase), a family of endoglycosidases that degrade HA into fragments with low molecular weights by cleaving its internal *β*-*N*-acetyl-D-glucosamine linkages. It has been reported that HAase is secreted by tumor cells and has a close relationship with the presence of tumors.[6,7] Specifically, the expressed levels of HAase increase in many tumor cells, such as bladder carcimoma,[6,7] prostate,[8,9] malignant melanoma,[10] and brain and neck cancer;[11,12] consequently, it is becoming a new type of tumor marker.[13−15] Therefore, sensitive detection of HAase is of vital importance for tumor diagnosis and therapy at its early stage.

A variety of methods for assaying HAase activity have been proposed. However, classical methods, such as turbidometry,[16] viscometry,[17] colorimetry,[18] and zymography,[19,20] either lack sensitivity and selectivity or need time-consuming prerequisite steps. Immunoassay is sensitive and selective but requires specialized and expensive reagents.[21,22] Moreover, most of these methods were only limited to in vitro detection in homogeneous solution. Alternatively, the fluorescence technique has been proved one of the most useful analytical tools in bioanalysis and bioimaging because it offers distinct advantages, such as high sensitivity, real-time response, and ease of use.[23,24] Some novel fluorescent probes have been recently designed for HAase detection by complexing or labeling HA with gold nanoparticles,[25,26] organic fluorescent dyes,[27−29] conjugated small molecules,[30] and upconversion luminescence material.[31] Although many of these fluorescence methods were superior to previous methods in terms of sensitivity, they are not without drawbacks. For instance, gold nanoparticles are apt to precipitate in biological high-salt environments,[32−34] and organic fluorescent dyes are not suitable for long-time observation due to photobleaching.[35] Some fluorescence methods may either suffer from poor specificity or require multiple covalent modifications at the free carboxyl groups of the HA substrate,[30,31] which could affect the activity of HA and HAase.[36] Furthermore, the activity of HAase has been seldom employed in fluorescence methods for tumor-targeting cell imaging and therapy. For instance, Ma et al. have developed a fluorescent probe for HAase detection and tumor-targeting

DOI: 10.1021/acsami.5b06799
ACS Appl. Mater. Interfaces 2015, 7, 21529−21537

imaging and phototherapy; nevertheless, triple covalent modifications of HA were involved in this methods.[25] Hence, for tumor diagnosis and therapy in biosystems based on HAase detection, there is still a great demand for novel HA-based fluorescent probes to improve the available methods with respect to their sensitivity, convenience, and reliability.

Thus, we developed a novel, simple, and sensitve method for HAase detection and tumor-targeting drug delivery and imaging, using a probe based on a fluorescent water-soluble conjugated polymer (WSCP)/hyaluronan-doxorubicin (HA-Dox) complex. In comparison with those small molecule fluorescent materials as mentioned above, WSCPs are known to show high fluorescence brightness, good photostability, and signal amplification properties due to their large, delocalized molecular structures.[37] They have established themselves as efficiently sensing platforms during the past decade,[37−45] and very recently, many have been proved useful for live-cell imaging because they exhibit low biotoxicity and their amphiphilic structures are suitable for cellular interaction and subsequent cellular entry.[46−50] Herein, a cationic conjugated polymer (CCP), PFEP, with good photostability was utilized in our method, which can form a complex with anionic HA conjugated with the model anticancer drug Dox (Scheme 1). Efficient electron transfer (ET) from PFEP to Dox (the quencher) occurred in the complex and triggered a "turn off" signal of PFEP.[51] When HAase was present, HA was degraded into small fragments and Dox was released, resulting in the obvious fluorescence recovery of PFEP.

Compared with other HAase assays, our work not only simplified the modification of the HA substrate but also provided high sensitivity with a detection limit of 0.075 U/mL. Moreover, this method allowed for rapid HAase detection. Simple mixing of fragmented HA-Dox (incubation within 30 min) and PFEP enabled HAase detection within 1 min. This fluorescent probe was also successfully used to detect the HAase levels in human urine samples. Furthermore, the PFEP/HA-Dox complex formed nanoparticles in aqueous solution, which can deliver Dox to targeted tumor cells via the overexpressed CD44 receptor, and subsequently image the cancer cells upon the degradation of HA by HAase. A multifunctional complex system for tumor diagnosis and therapy was thus constructed.

EXPERIMENTAL SECTION

Materials and Instruments. The water-soluble cationic conjugated polymer poly{[9,9-bis(6′-(*N*,*N*,*N*-diethylmethylammonium)-hexyl)-2,7-fluorenylene ethynylene]-*alt*-*co*-[2,5-bis(3′-(*N*,*N*,*N*-diethylmethylammonium)-1′-oxapropyl)-1,4-phenylene]} tetraiodide (PFEP) was synthesized according to a previously reported method.[52] The molecular weight and polydispersity of its neutral polymer are 12600 and 1.28, respectively.

Sodium hyaluronate (60 kDa) was purchased from Mellon Biological Technology Co., Ltd. (Dalian, China). Doxorubicin hydrochloride (Dox·HCl) was purchased from Aladdin (Shanghai, China). Hyaluronidase, ribonuclease A, trypsin, thrombin, and lysozyme were ordered from Sigma. *N*-Hydroxysuccinimide (NHS) was purchased from Acros organics. 1-(3-(Dimethylamino)propyl)-3-ethylcarbodiimide hydrochloride (EDC) was purchased from TCI. Human urine specimens were obtained from Zhongda Hospital (Nanjing, China). All other reagents were obtained from Sinopharm Chemical Reagent Co., Ltd. (Shanghai, China). All solutions were prepared using Milli-Q water (18.2 MΩ cm) from a Millipore system.

UV−vis absorption spectra were recorded on a SHIMADZU UV-3600 spectrophotometer. Photoluminescence (PL) measurements were carried out using a SHIMADZU RF-5301PC spectrofluorophotometer with a xenon lamp as a light source. Transmission electron microscopy (TEM) images were obtained with a JEOL 2010 transmission electron microscope at an accelerating voltage of 100 kV. Fluorescence images were recorded on a confocal laser scanning microscope (CLSM, Leica, TCS SP5, Germany).

Methods. *Preparation and Characterization of HA-Dox Conjugates.* HA (50 mg, 0.12 mmol of disaccharide repeating units) was dissolved in a 10 mL mixture of DMSO and H_2O. Then, 0.7 mL of 20 mg/mL EDC (14 mg, 0.07 mmol) aqueous solution was added to the above solution, and the mixture was stirred for about 10−15 min. Then, 1.8 mL of 10 mg/mL NHS (18 mg, 0.16 mmol) aqueous solution was added. Finally, Dox·HCl (5 mg, 0.0086 mmol) was added, and the mixture was stirred at room temperature for 24 h. The reaction mixture was dialyzed using a membrane with molecular cutoff of 3500 for 5 days to remove the unreacted Dox·HCl, EDC, and NHS. Then, the HA-Dox sample was stored as the lyophilized solid in the absence of light at −20 °C.

Detection of Hyaluronidase (HAase). For the detection of HAase, fluorescence spectrometric titration experiments were carried out at room temperature (25 °C) in a 700 μL quartz cuvette. HAase (1−10 μL, 100 U/mL) dissolved in a phosphate buffered saline (PBS, 0.02 M, 0.15 M NaCl, pH 5.6) was added to 2 μL of HA-Dox ([HA-Dox] = 4.0×10^{-4} M) in Milli-Q water, and then 10 μL of PBS was added to the solution. After incubation at 37 °C for 30 min, the mixed solution was diluted to 540 uL with PBS buffer, and PFEP was added ([PFEP] = 1.5×10^{-7} M; the concentrations all refer to the molar concentrations of the polymer repeat unit). Then, the fluorescence spectra were recorded with an excitation of 405 nm.

Determination of HAase in Urine Specimens. Detection of HAase in human urine specimens from 12 healthy people was performed as follows. First, 200 μL of each urine sample was mixed properly with 30 mg of chitosan and then centrifuged at 10000 r/min for 10 min (according to the literatures, chitosan was used to agglomerate all negatively charged moieties in urine samples without adsorbing HAase molecules).[12,30] Then, the urine supernatant was added into the probe solution, and the fluorescence was measured according to the same procedure as described above. The final concentration of the urine in the test solutions was 54-fold diluted.

Preparation and Characterization of PFEP/HA-Dox Nanoprobes Used in Cell Imaging. HA-Dox (360 μL, [HA-Dox] = 5.0×10^{-4} M) was dissolved in 50 mL of Milli-Q water in a beaker under stirring at room temperature, and the solution was sonicated. Then, 1 mL of PFEP ([PFEP] = 5.0×10^{-5} M) methanol solution was added dropwise slowly to the above solution. The solution was lyophilized for 3 days to afford PFEP/HA-Dox nanoprobes as a solid. For the TEM analysis, each drop of the PFEP/HA-Dox complex solutions was placed on a 200 mesh copper grid with a carbon film, air-dried, and analyzed with a TEM.

Cellular Uptake of PFEP/HA-Dox Complex and Imaging. We tracked the cellular internalization of PFEP/HA-Dox nanoprobes in Hela cells (cancer cell) and NIH-3T3 cells (normal cell) to evaluate the cancer cell specificity. First, the cells were cultured in confocal microscope dishes at a density of 5×10^5/mL in culture medium for 24 h at 37 °C. Then, the medium was replaced with the medium without FBS and containing the above PFEP/HA-Dox nanoprobes. The final concentrations of PFEP and HA-Dox were 2.0×10^{-5} M and 5.6×10^{-5} M, respectively. After incubation for 3 h at 37 °C, the cells were rinsed twice with PBS (0.01 M, pH 7.4). As a control experiment, another dish of Hela cells was incubated with a high dose of free-HA ([HA] = 3 mg/mL) for 2 h at 37 °C before treatment with the PFEP/HA-Dox complex. The fluorescent images were all recorded on a confocal laser scanning microscope with excitation at 405 and 488 nm, and the emissions in the ranges of 430−460 nm and 520−600 nm were recorded, respectively.

RESULTS AND DISCUSSION

Preparation and Characterization. Dox was covalently conjugated to the HA backbone using the conventional EDC chemistry.[53] HA-Dox was purified by dialysis using a membrane

DOI: 10.1021/acsami.5b06799
ACS Appl. Mater. Interfaces 2015, 7, 21529−21537

with a molecular cutoff of 3500 for 5 days. The degree of substitution (DS, defined as the weight content of Dox in HA-Dox) was determined using a Dox absorption standard curve, and it was assayed to be about 5.7%.[51] The absorption and emission spectra of PFEP and HA-Dox are shown in Figure 1.

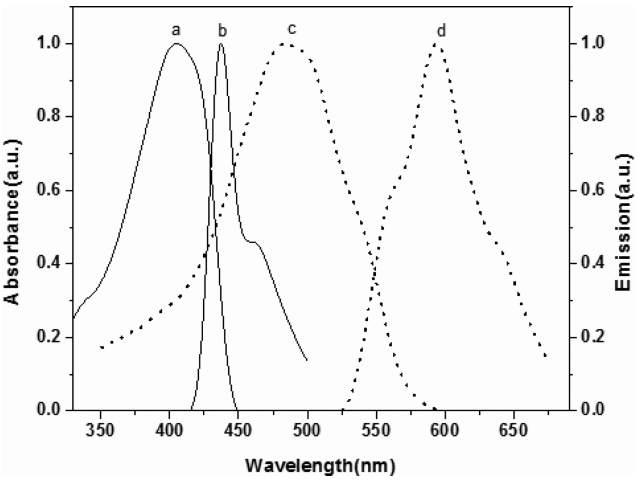

Figure 1. UV−vis absorption (a, c) and emission spectra (b, d) of PFEP (a, b) and HA-Dox (c, d) in PBS buffer solution (0.02 M, pH 5.6).

The absorption spectrum of PFEP showed a maximum peak at 405 nm. Upon excitation at 405 nm, the emission spectrum exhibited a maximum peak at 445 nm. PFEP displayed stable blue light emission in water with a high quantum yield of 26%.[49,52]

Detection of HAase. The strategy for HAase detection is illustrated in Scheme 1a. The negatively charged HA-Dox can form a complex with cationic PFEP through electrostatic interactions. As shown in Scheme 1b, the PFEP/HA-Dox complex consisted of three components: (1) water-soluble cationic conjugated polymer PFEP for fluorescence imaging, (2) HA as drug carrier that can be cleaved by HAase to release the covalent linking drug, and (3) Dox, which is one of the most effective chemotherapeutic anticancer drugs for various tumors. Dox contains one quinone group that is a highly efficient electron transfer (ET) quencher.[54,55] Thus, the close proximity between PFEP and Dox in the PFEP/PG-Dox complex allowed for efficient quenching of PFEP by Dox. Upon adding HAase, HA was degraded into small fragments, and the electrostatic interactions of HA fragments with PFEP were relatively weak. In this case, Dox was released and became far away from PFEP, so the fluorescence of PFEP was recovered. By monitoring the change of emission intensity of PFEP with the addition of HAase, it was possible to detect HAase quantitatively.

First, we did the following experiments to verify that the strategy was feasible. As shown in Figure 2a, PFEP itself ([PFEP] = 1.5×10^{-7} M) in PBS (0.02 M, pH = 5.6; previous studies have shown that the activity of HAase is optimal in a weak acidic environment)[12,30,56] emitted strong fluorescence with a maximum at 445 nm when excited at 405 nm. The addition of HA-Dox ([Dox] = 6.39×10^{-8} M) to the solution of PFEP led to an efficient fluorescence quenching due to the electron transfer from PFEP to Dox. Additionally, the electrostatic attraction in the PFEP/HA-Dox complex would induce interchain aggregation of PFEP, which was also believed

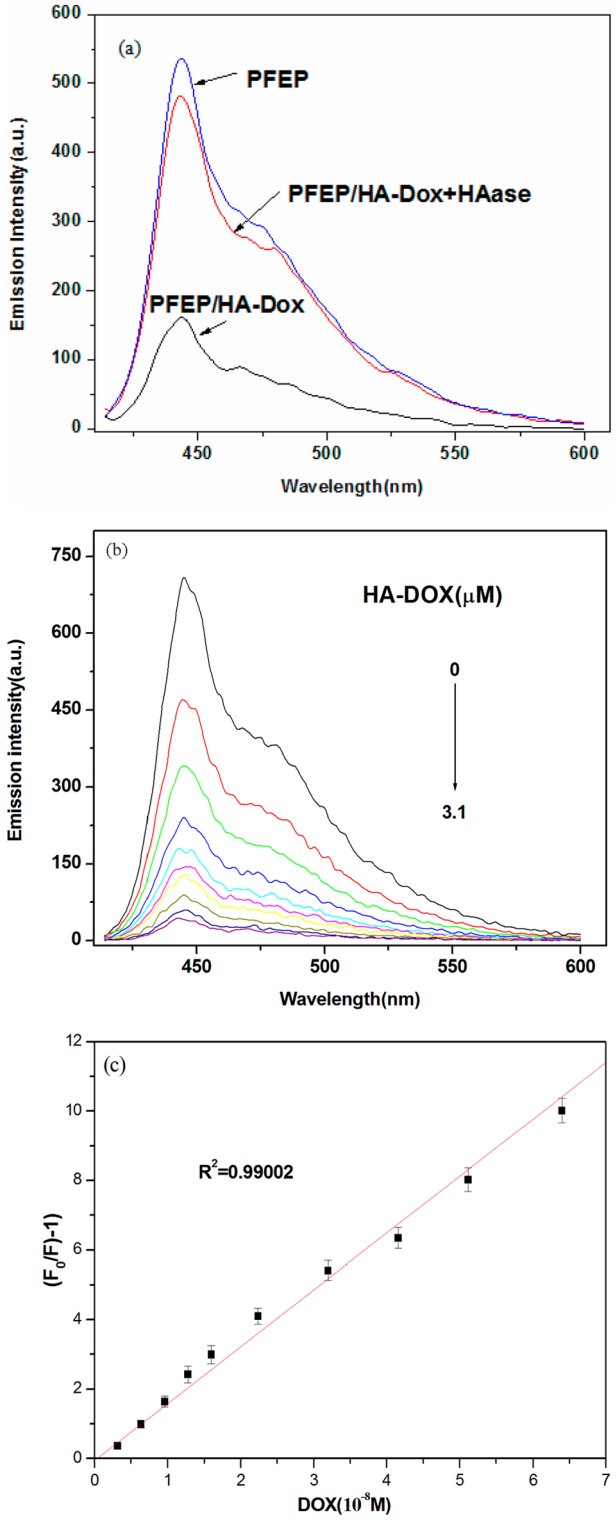

Figure 2. (a) Emission spectra of PFEP, PFEP/HA-Dox complex before and after treatment with HAase for 30 min at 37 °C. [PFEP] = 1.5×10^{-7} M, [Dox] = 6.39×10^{-8} M, [HAase] = 1.30 U/mL. (b) Fluorescence emission spectra of PFEP with successive additions of HA-Dox. (c) K_{sv} plot of PFEP in the presence of HA-Dox. [PFEP] = 1.5×10^{-7} M, [Dox] = 0−6.39×10^{-8} M.

to contribute partly to the quenching of conjugated polymer.[52] After the addition of HAase ([HAase] = 1.30 U/mL) and the subsequent incubation for 30 min at 37 °C, 89% fluorescence of PFEP was recovered because of the hydrolysis of HA, which

DOI: 10.1021/acsami.5b06799
ACS Appl. Mater. Interfaces 2015, 7, 21529−21537

made the quencher Dox far away from PFEP. Further addition of HAase cannot make the fluorescence of PFEP recover completely, which may also indicate the quenching effect of PFEP due to the aggregation induced by the residual weak electrostatic interactions between PFEP and HA fragments.

Then, to determine the efficiency of fluorescence quenching, we examined the Stern−Volmer constant (K_{sv}) by monitoring measurable fluorescence changes of PFEP using the Stern−Volmer equation, where F_0 and F are the emission intensities of PFEP in the absence and presence of the HA-Dox, respectively, and [Q] is the concentration of the quencher Dox.[57]

$$F_0/F = 1 + K_{sv}[Q]$$

As shown in Figure 2b, the fluorescence of PFEP was gradually quenched with the successive addition of HA-Dox. A linear Stern−Volmer plot was obtained with a K_{sv} value of 1. 62 × 10^8 M^{-1} (Figure 2c).

Figure 3a shows the fluorescence intensity changes of PFEP/HA-Dox ([PFEP] = 1.5 × 10^{-7} M, [Dox] = 6.39 × 10^{-8} M) with the increase of HAase concentration that ranged from 0 to 1.85 U/mL. The initial solution of the PFEP/HA-Dox complex displayed a weak emission of PFEP. The emission intensity of PFEP gradually rose with the increase of HAase concentration and was almost recovered at the concentration of 1.85 U/mL. We also examined the degree of fluorescence recovery using ΔI calculated from the following equation, where I_0 and I_C are the emission intensities of PFEP in the absence and presence of HAase, respectively.

$$\Delta I = I_C/I_0$$

The dependence of ΔI as a function of HAase concentration is shown in Figure 3b. The inset of Figure 3b shows that ΔI was linearly correlated with the concentration of the HAase from 0 to 1.30 U/mL. Thus, the limit of detection (LOD) was estimated to be 0.075 U/mL at a signal-to-noise ratio of 3. This result showed better performance than most classical methods[16−20] and recently developed fluorescence methods[25−29] for assaying HAase activity.

Furthermore, in order to explore more fully the specificity of this strategy for HAase detection, a series of control experiments were conducted using thrombin, lysozyme, ribonuclease, and trypsin. The results shown in Figure 3c indicated that the addition of thrombin, lysozyme, ribonuclease, trypsin, and PBS did not produce the high ΔI observed for HAase, even though the concentration of the former (9.3 U/mL) was more than 5 times that of the latter (1.85 U/mL). This finding further confirmed that the enzyme that did not cleave HA would not weaken the electrostatic interactions between PFEP and HA-Dox; hence, the efficient electron transfer would be maintained and ΔI was very low. Additionally, blank experiment was also done using PBS. PBS with the same volume as that of HAase was added to the solution of PFEP/HA-Dox, and a very low ΔI was obtained, implying that the dilution of the solution did not have much effect on the results of detection.

The above work studied the sensitivity and specificity of the PFEP/HA-Dox complex for HAase analysis in a buffer system. Furthermore, the PFEP/HA-Dox complex was used to detect HAase in human urine specimens to explore their practical application. Table 1 shows that the concentrations of HAase in the urine specimens from 12 normal healthy people were between 2.28 and 24.81 U/mL,[26] which is in agreement with the previous findings of HAase level for other normal healthy people.

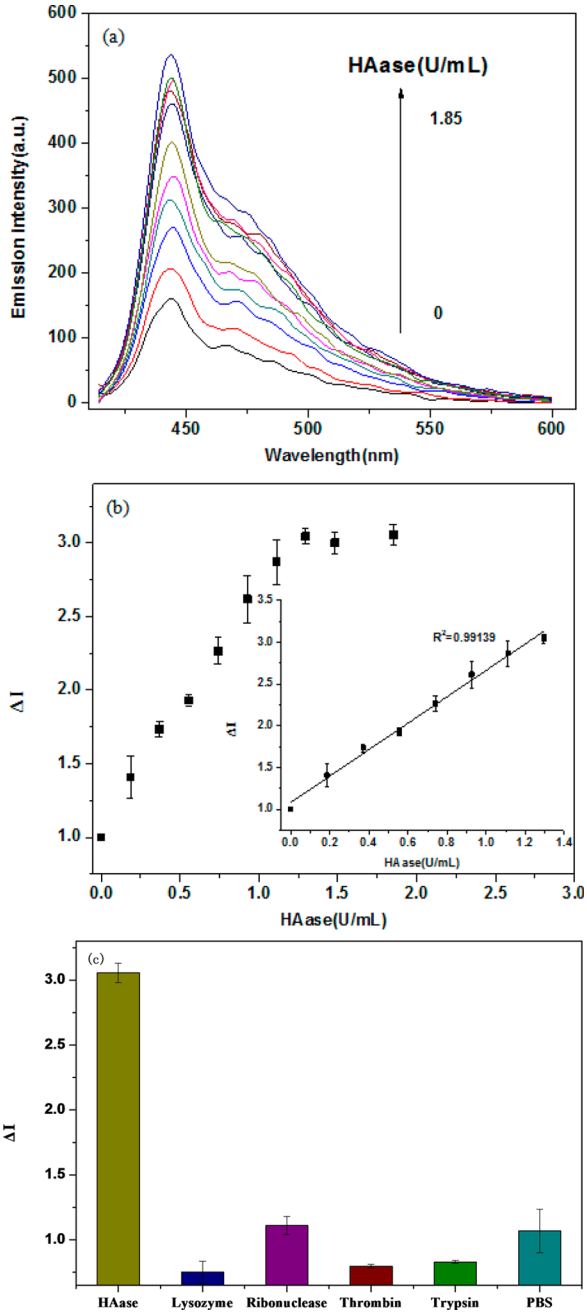

Figure 3. (a) Emission spectra of PFEP/HA-Dox complex with increasing concentration of HAase. [HAase] = 0−1.85 U/mL. (b) Dependence of ΔI as a function of HAase concentration. The inset shows the linear plot obtained in the concentration range from 0 to 1.30 U/mL. (c) Comparison of the ΔI for the detection of HAase (1.85 U/mL) and other enzymes (thrombin, lysozyme, ribonuclease, trypsin, and PBS, each at 9.3 U/mL). Measurements were performed in PBS (0.02 M, pH 5.6). [PFEP] = 1.5 × 10^{-7} M, [Dox] = 6.39 × 10^{-8} M.

Tumor-Targeting Drug Delivery and Cell Imaging. Moreover, we also studied in vitro Dox release of PFEP/HA-Dox complex in the presence of HAase. Figure 4a shows the dependence of emission intensity of the PFEP/HA-Dox complex as a function of HAase digestion time. After adding HAase ([HAase] = 1.30 U/mL), the fluorescence of PFEP

DOI: 10.1021/acsami.5b06799
ACS Appl. Mater. Interfaces 2015, 7, 21529−21537

Table 1. Detection of HAase in Human Urine Specimens by Using PFEP/HA-Dox Complex

numbers	1	2	3	4	5	6	7	8	9	10	11	12
found (U mL^{-1})	8.03	13.73	2.28	12.93	7.67	8.34	15.02	24.81	24.04	3.20	8.50	9.28

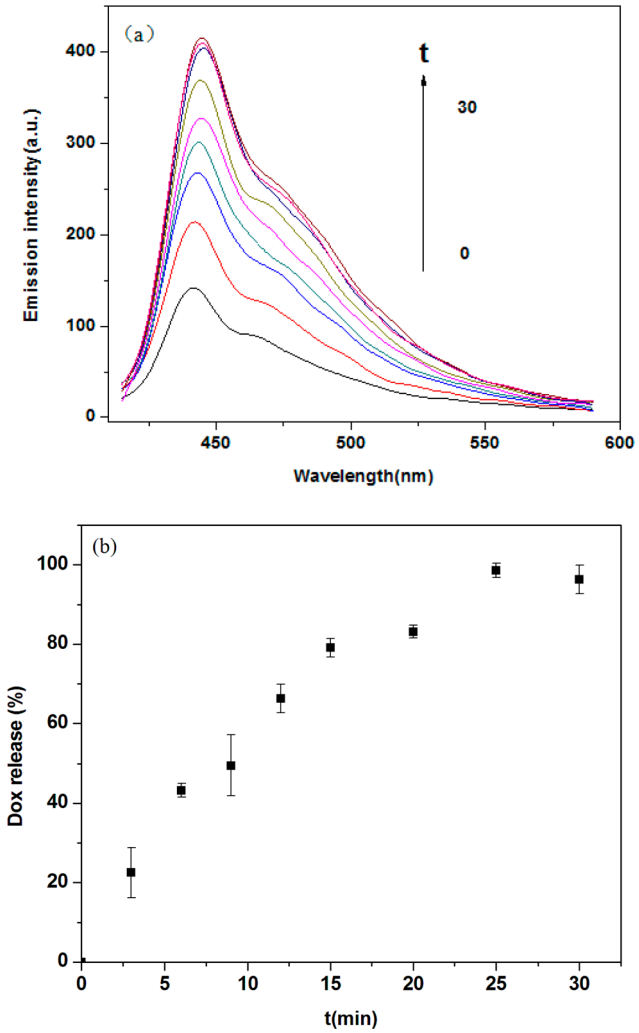

Figure 4. (a) Emission intensity of PFEP/HA-Dox complex as a function of HAase digestion time. [Dox] = 6.39×10^{-8} M, [HAase] = 1.30 U/mL, [PFEP] = 1.5×10^{-7} M. (b) Dependence of Dox release as a function of HAase digestion time.

increased gradually as the digestion time went on from 0 to 25 min and remained almost unchanged after 25 min. For the PFEP/HA-Dox complex in the presence of HAase, the concentration of Dox at different times can be calculated from the fluorescence intensity of PFEP from the Stern−Volmer curve to calculate the drug release efficiency. As shown in Figure 4b, the anticancer drug Dox was released quickly at the first 15 min and gradually reached a plateau after 25 min. Thus, we can monitor the Dox release quantitatively based on the fluorescence "turn-on" signal of PFEP.

The results obtained from in vitro Dox release studies motivated us to further investigate the uptake of the PFEP/HA-Dox complex into tumor cells. HA can specifically bind to the receptor, CD44, a major adhesion protein that is overexpressed on various kinds of cancer cells.[1−5] Moreover, it was reported that the expression of HAase was positively correlated with tumor malignancies and suggested to be a marker of tumorigenesis.[13−15] Therefore, our method provided the possibility of diagnosis and therapy of cancer through tumor-targeting cell imaging and drug delivery.

First, we prepared PFEP/HA-Dox nanoparticles used in the cell experiments. As shown in Figure 5, the PFEP/HA-Dox

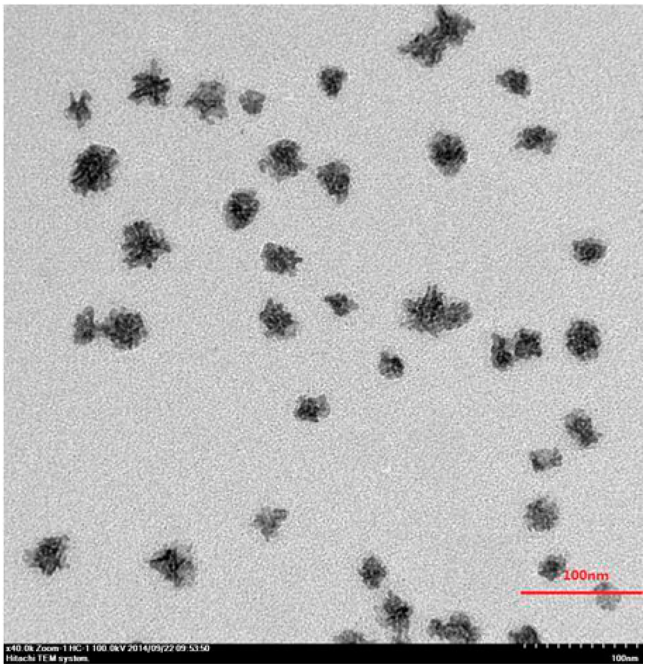

Figure 5. TEM images of the nanoparticles formed by PFEP/HA-Dox complex (scale bar: 100 nm).

complex formed nanoparticles in PBS with the sizes of 30−50 nm, and the nanoparticles were well-dispersed. Then, we evaluated the cellular uptake efficiency with PFEP/HA-Dox nanoparticles by CLSM studies in NIH-3T3 cells (mouse embryonic fibroblast cell) and Hela cells (human cervical cancer cell). It has been previously reported that NIH3T3 is a normal cell line with low CD44 expression[58] and that Hela is a cancer cell line with high CD44 expression.[59] As shown in Figure 6a, fluorescent signals are clearly observed in the cytoplasm for Hela cells, indicating that PFEP/HA-Dox nanoparticles were readily internalized into Hela cells via CD44-mediated endocytosis because of specific HA−CD44 binding. The blue color with excitation at 405 nm should be attributed to the recovery of emission from PFEP, and the red color with excitation at 488 nm should come from the emission of Dox, because the HAase overexpressed mainly in the cytoplasm of cancer cells degraded HA and Dox was released from the complex in the weak acidic environment.[25,51,60] In comparison, when the Hela cells were pretreated with a high dose of free-HA to block CD44 before PFEP/HA-Dox complex treatment, intracellular fluorescence was rarely observed in Figure 6b, implying a lack of cellular uptake of PFEP/HA-Dox nanoparticles. Also, when the PFEP/HA-Dox complex was incubated with NIH-3T3 cells, which displayed low CD44 expression, only very weak signals were observed in Figure 6c. This indicated that the polymer was mainly taken up by the cell as part of the complex because the specific HA−CD44 binding

DOI: 10.1021/acsami.5b06799
ACS Appl. Mater. Interfaces 2015, 7, 21529−21537

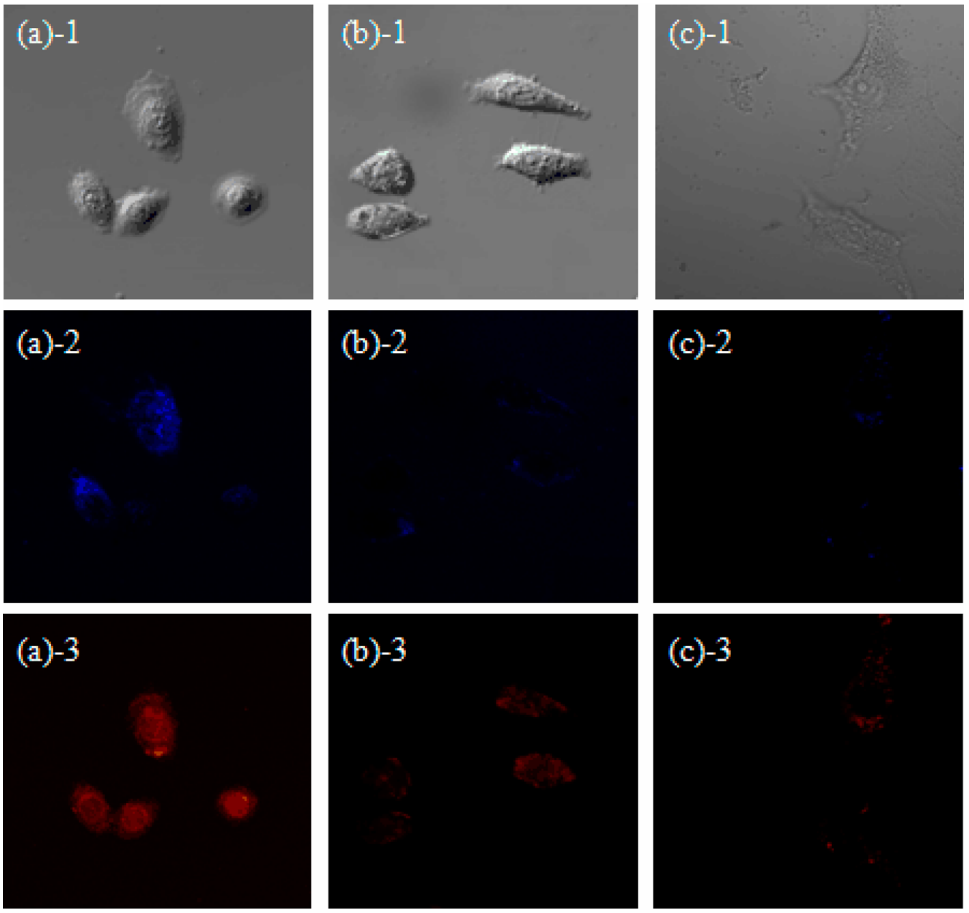

Figure 6. Phase contrast images (1) and fluorescent microscopic (2−3) images of Hela cells (a), Hela cells pretreated with HA (b), and NIH-3T3 cells (c) after incubation with PFEP/HA-Dox complex for 3 h at 37 °C.

helped to improve the cellular uptake efficiency. All of the above results demonstrated the multifunctionality of the PFEP/HA-Dox complex system, which can not only deliver Dox to the targeted tumor cells and monitor the Dox release based on the fluorescence "turn-on" signal of PFEP but also simultaneously imaged the targeted tumor cells with good photostability.

CONCLUSION

In summary, a novel fluorescent probe, PFEP/HA-Dox complex, for sensitive, rapid, and convenient HAase detection was developed. In contrast to previously reported methods, this probe was easy to fabricate because it only required a single modification of HA through a mature reaction. The simple modification of HA (reducing the influence on the activity of HAase), combined with the excellent optoelectronic property of PFEP, gave rise to the high specificity and high sensitivity with the detection limit of 0.075 U/mL as well as a shortened detection time. Our method has a shorter turnaround time (30 min) compared to zymography (48 h)[19,20] and most previous methods (close to or more than 1 h).[26−31] Importantly, quantitative measurements of the HAase activity in human urine samples were also successfully conducted. Furthermore, through the specific HA−CD44 binding and the degradation of HA by HAase in tumor cells, the PFEP/HA-Dox complex can be employed as a multifunctional system by realizing tumor-targeting drug delivery and cell imaging simultaneously. The present work may offer a promising approach for early tumor diagnosis and therapy based on HAase detection.

AUTHOR INFORMATION

Corresponding Authors

*E-mail: iamyqhuang@njupt.edu.cn. Tel: +86 25 8586 6396. Fax: +86 25 8586 6396 (Y.H.).
*E-mail: zhangpeter1100@163.com (R.Z.).
*E-mail: wei-huang@njtech.edu.cn. Fax: +86 25 5813 9988. Tel: +86 25 5813 9001 (W.H.).

Notes

The authors declare no competing financial interest.

ACKNOWLEDGMENTS

The authors gratefully thank the National Basic Research Program of China (Nos. 2009CB930601, 2012CB933301, 2012CB723402), the National Natural Science Foundation of China (Nos. 51073078, 21005040, 51173081, 51273092), the Natural Science Foundation of Jiangsu Province, China (BM2012010), the Science Foundation of Nanjing University of Posts and Telecommunications (NY213173), the Ministry of Education of China (No. IRT1148), the Priority Academic Program Development of Jiangsu Higher Education Institutions (PAPD), and the Synergetic Innovation Center for Organic Electronics and Information Displays for the financial support.

DOI: 10.1021/acsami.5b06799
ACS Appl. Mater. Interfaces 2015, 7, 21529−21537

REFERENCES

(1) Lapcik, L.; Lapcik, L.; De Smedt, S.; Demeester, J.; Chabrecek, P. Hyaluronan: Preparation, Structure, Properties, and Applications. *Chem. Rev.* **1998**, *98*, 2663−2684.

(2) Lokeshwar, V. B.; Selzer, M. G. Hyalurondiase: Both a Tumor Promoter and Suppressor. *Semin. Cancer Biol.* **2008**, *18*, 281−287.

(3) Ikegami-Kawai, M.; Takahashi, T. Microanalysis of Hyaluronan Oligosaccharides by Polyacrylamide Gel Electrophoresis and Its Application to Assay of Hyaluronidase Activity. *Anal. Biochem.* **2002**, *311*, 157−165.

(4) Toole, B. P. Hyaluronan: From Extracellular Glue to Pericellular Cue. *Nat. Rev. Cancer* **2004**, *4*, 528−539.

(5) Turley, E. A.; Noble, P. W.; Bourguignon, L. Y. W. Signaling Properties of Hyaluronan Receptors. *J. Biol. Chem.* **2002**, *277*, 4589−4592.

(6) Whatcott, C. J.; Han, H.; Posner, R. G.; Hostetter, G.; Von Hoff, D. D. Targeting the Tumor Microenvironment in Cancer: Why Hyaluronidase Deserves a Second Look. *Cancer Discovery* **2011**, *1*, 291−296.

(7) Tan, J.-X.; Wang, X.-Y.; Li, H.-Y.; Su, X.-L.; Wang, L.; Ran, L.; Zheng, K.; Ren, G.-S. Hyal1 Overexpression Is Correlated with the Malignant Behavior of Human Breast Cancer. *Int. J. Cancer* **2011**, *128*, 1303−1315.

(8) Lokeshwar, V. B.; Rubinowicz, D.; Schroeder, G. L.; Forgacs, E.; Minna, J. D.; Block, N. L.; Nadji, M.; Lokeshwar, B. L. Stromal and Epithelial Expression of Tumor Markers Hyaluronic Acid and Hyal1 Hyaluronidase in Prostate Cancer. *J. Biol. Chem.* **2001**, *276*, 11922−11932.

(9) Benitez, A.; Yates, T. J.; Lopez, L. E.; Cerwinka, W. H.; Bakkar, A.; Lokeshwar, V. B. Targeting Hyaluronidase for Cancer Therapy: Antitumor Activity of Sulfated Hyaluronic Acid in Prostate Cancer Cells. *Cancer Res.* **2011**, *71*, 4085−4095.

(10) Liu, D. C.; Pearlman, E.; Diaconu, E.; Guo, K.; Mori, H.; Haqqi, T.; Markowitz, S.; Willson, J.; Sy, M. S. Expression of Hyaluronidase by Tumor Cells Induces Angiogenesis in Vivo. *Proc. Natl. Acad. Sci. U. S. A.* **1996**, *93*, 7832−7837.

(11) Martinez-Quintanilla, J.; He, D.; Wakimoto, H.; Alemany, R.; Shah, K. Encapsulated Stem Cells Loaded with Hyaluronidase-Expressing Oncolytic Virus for Brain Tumor Therapy. *Mol. Ther.* **2015**, *23*, 108−118.

(12) Nossier, A. I.; Eissa, S.; Ismail, M. F.; Hamdy, M. A.; Azzazy, H. M. E.-S. Direct Detection of Hyaluronidase in Urine Using Cationic Gold Nanoparticles: A Potential Diagnostic Test for Bladder Cancer. *Biosens. Bioelectron.* **2014**, *54*, 7−14.

(13) Kim, J.-W.; Kim, J. H.; Chung, S. J.; Chung, B. H. An Operationally Simple Colorimetric Assay of Hyaluronidase Activity Using Cationic Gold Nanoparticles. *Analyst* **2009**, *134*, 1291−1293.

(14) Posey, J. T.; Soloway, M. S.; Ekici, S.; Sofer, M.; Civantos, F.; Duncan, R. C.; Lokeshwar, V. B. Evaluation of the Prognostic Potential of Hyaluronic Acid and Hyaluronidase (Hyal1) for Prostate Cancer. *Cancer Res.* **2003**, *63*, 2638−2644.

(15) Franzmann, E. J.; Schroeder, G. L.; Goodwin, W. J.; Weed, D. T.; Fisher, P.; Lokeshwar, V. B. Expression of Tumor Markers Hyaluronic Acid and Hyaluronidase (Hyal1) in Head and Neck Tumors. *Int. J. Cancer* **2003**, *106*, 438−445.

(16) Di Ferrante, N. Turbidimetric Measurement of Acid Mucopolysaccharides and Hyaluronidase Activity. *J. Biol. Chem.* **1956**, *220*, 303−306.

(17) Balazs, E. A.; Von Euler, J. The Hyaluronidase Content of Necrotic Tumor and Testis Tissue. *Cancer Res.* **1952**, *12*, 326−329.

(18) Bonner, W. M., Jr.; Cantey, E. Y. Colorimetric Method for Determination of Serum Hyaluronidase Activity. *Clin. Chim. Acta* **1966**, *13*, 746−752.

(19) Steiner, B.; Cruce, D. A Zymographic Assay for Detection of Hyaluronidase Activity on Polyacrylamide Gels and Its Application to Enzymatic-Activity Found in Bacteria. *Anal. Biochem.* **1992**, *200*, 405−410.

(20) Magalhaes, M. R.; da Silva, N. J., Jr.; Ulhoa, C. J. A Hyaluronidase from Potamotrygon Motoro (Freshwater Stingrays) Venom: Isolation and Characterization. *Toxicon* **2008**, *51*, 1060−1067.

(21) Stern, M.; Stern, R. An Elisa-Like Assay for Hyaluronidase and Hyaluronidase Inhibitors. *Matrix* **1992**, *12*, 397−403.

(22) Delpech, B.; Bertrand, P.; Maingonnat, C.; Girard, N.; Chauzy, C. Enzyme-Linked Hyaluronectin - a Unique Reagent for Hyaluronan Assay and Tissue Location and for Hyaluronidase Activity Detection. *Anal. Biochem.* **1995**, *229*, 35−41.

(23) Giepmans, B. N. G.; Adams, S. R.; Ellisman, M. H.; Tsien, R. Y. Review - the Fluorescent Toolbox for Assessing Protein Location and Function. *Science* **2006**, *312*, 217−224.

(24) Alivisatos, A. P.; Gu, W. W.; Larabell, C. Quantum Dots as Cellular Probes. *Annu. Rev. Biomed. Eng.* **2005**, *7*, 55−76.

(25) Song, Y.; Wang, Z.; Li, L.; Shi, W.; Li, X.; Ma, H. Gold Nanoparticles Functionalized with Cresyl Violet and Porphyrin Via Hyaluronic Acid for Targeted Cell Imaging and Phototherapy. *Chem. Commun.* **2014**, *50*, 15696−15698.

(26) Cheng, D.; Han, W.; Yang, K.; Song, Y.; Jiang, M.; Song, E. One-Step Facile Synthesis of Hyaluronic Acid Functionalized Fluorescent Gold Nanoprobes Sensitive to Hyaluronidase in Urine Specimen from Bladder Cancer Patients. *Talanta* **2014**, *130*, 408−414.

(27) Zhang, L.-S.; Mummert, M. E. Development of a Fluorescent Substrate to Measure Hyaluronidase Activity. *Anal. Biochem.* **2008**, *379*, 80−85.

(28) Fudala, R.; Mummert, M. E.; Gryczynski, Z.; Gryczynski, L. Fluorescence Detection of Hyaluronidase. *J. Photochem. Photobiol., B* **2011**, *104*, 473−477.

(29) Rich, R. M.; Mummert, M.; Foldes-Papp, Z.; Gryczynski, Z.; Borejdo, J.; Gryczynski, I.; Fudala, R. Detection of Hyaluronidase Activity Using Fluorescein Labeled Hyaluronic Acid and Fluorescence Correlation Spectroscopy. *J. Photochem. Photobiol., B* **2012**, *116*, 7−12.

(30) Xie, H.; Zeng, F.; Wu, S. Ratiometric Fluorescent Biosensor for Hyaluronidase with Hyaluronan as Both Nanoparticle Scaffold and Substrate for Enzymatic Reaction. *Biomacromolecules* **2014**, *15*, 3383−3389.

(31) Wang, Z.; Li, X.; Song, Y.; Li, L.; Shi, W.; Ma, H. An Upconversion Luminescence Nanoprobe for the Ultrasensitive Detection of Hyaluronidase. *Anal. Chem.* **2015**, *87*, 5816−5823.

(32) Huang, C.-C.; Chiang, C.-K.; Lin, Z.-H.; Lee, K.-H.; Chang, H.-T. Bioconjugated Gold Nanodots and Nanoparticles for Protein Assays Based on Photoluminescence Quenching. *Anal. Chem.* **2008**, *80*, 1497−1504.

(33) Ai, K.; Liu, Y.; Lu, L. Hydrogen-Bonding Recognition-Induced Color Change of Gold Nanoparticles for Visual Detection of Melamine in Raw Milk and Infant Formula. *J. Am. Chem. Soc.* **2009**, *131*, 9496−9497.

(34) Xue, J.; Shan, L.; Chen, H.; Li, Y.; Zhu, H.; Deng, D.; Qian, Z.; Achilefu, S.; Gu, Y. Visual Detection of Stat5b Gene Expression in Living Cell Using the Hairpin DNA Modified Gold Nanoparticle Beacon. *Biosens. Bioelectron.* **2013**, *41*, 71−77.

(35) Yang, J.; Zhang, Y.; Gautam, S.; Liu, L.; Dey, J.; Chen, W.; Mason, R. P.; Serrano, C. A.; Schug, K. A.; Tang, L. Development of Aliphatic Biodegradable Photoluminescent Polymers. *Proc. Natl. Acad. Sci. U. S. A.* **2009**, *106*, 10086−10091.

(36) Hu, J.; Zhang, G.; Liu, S. Enzyme-Responsive Polymeric Assemblies, Nanoparticles and Hydrogels. *Chem. Soc. Rev.* **2012**, *41*, 5933−5949.

(37) Thomas, S. W., III; Joly, G. D.; Swager, T. M. Chemical Sensors Based on Amplifying Fluorescent Conjugated Polymers. *Chem. Rev.* **2007**, *107*, 1339−1386.

(38) Feng, X.; Liu, L.; Wang, S.; Zhu, D. Water-Soluble Fluorescent Conjugated Polymers and Their Interactions with Biomacromolecules for Sensitive Biosensors. *Chem. Soc. Rev.* **2010**, *39*, 2411−2419.

(39) Jiang, H.; Taranekar, P.; Reynolds, J. R.; Schanze, K. S. Conjugated Polyelectrolytes: Synthesis, Photophysics, and Applications. *Angew. Chem., Int. Ed.* **2009**, *48*, 4300−4316.

DOI: 10.1021/acsami.5b06799
ACS Appl. Mater. Interfaces 2015, 7, 21529−21537

(40) Ho, H.-A.; Najari, A.; Leclerc, M. Optical Detection of DNA and Proteins Moth Cationic Polythiophenes. *Acc. Chem. Res.* **2008**, *41*, 168−178.
(41) Liu, B.; Bazan, G. C. Homogeneous Fluorescence-Based DNA Detection with Water-Soluble Conjugated Polymers. *Chem. Mater.* **2004**, *16*, 4467−4476.
(42) Li, J.; Huang, Y.-Q.; Qin, W.-S.; Liu, X.-F.; Huang, W. An Optical-Logic System Based on Cationic Conjugated Polymer/DNA/Intercalating Dyes Assembly for Label-Free Detection of Conformational Conversion of DNA I-Motif Structure. *Polym. Chem.* **2011**, *2*, 1341−1346.
(43) Huang, Y.-Q.; Liu, X.-F.; Fan, Q.-L.; Wang, L.; Song, S.; Wang, L.-H.; Fan, C.; Huang, W. Tuning Backbones and Side-Chains of Cationic Conjugated Polymers for Optical Signal Amplification of Fluorescent DNA Detection. *Biosens. Bioelectron.* **2009**, *24*, 2973−2978.
(44) Liu, X.; Shi, L.; Hua, X.; Huang, Y.; Su, S.; Fan, Q.; Wang, L.; Huang, W. Target-Induced Conjunction of Split Aptamer Fragments and Assembly with a Water-Soluble Conjugated Polymer for Improved Protein Detection. *ACS Appl. Mater. Interfaces* **2014**, *6*, 3406−3412.
(45) Liu, X.; Ouyang, L.; Cai, X.; Huang, Y.; Feng, X.; Fan, Q.; Huang, W. An Ultrasensitive Label-Free Biosensor for Assaying of Sequence-Specific DNA-Binding Protein Based on Amplifying Fluorescent Conjugated Polymer. *Biosens. Bioelectron.* **2013**, *41*, 218−224.
(46) Zhu, C.; Liu, L.; Yang, Q.; Lv, F.; Wang, S. Water-Soluble Conjugated Polymers for Imaging, Diagnosis, and Therapy. *Chem. Rev.* **2012**, *112*, 4687−4735.
(47) Pu, K.-Y.; Liu, B. Fluorescent Conjugated Polyelectrolytes for Bioimaging. *Adv. Funct. Mater.* **2011**, *21*, 3408−3423.
(48) Parthasarathy, A.; Ahn, H.-Y.; Belfield, K. D.; Schanze, K. S. Two-Photon Excited Fluorescence of a Conjugated Polyelectrolyte and Its Application in Cell Imaging. *ACS Appl. Mater. Interfaces* **2010**, *2*, 2744−2748.
(49) Huang, Y.; Yao, X.; Zhang, R.; Ouyang, L.; Jiang, R.; Liu, X.; Song, C.; Zhang, G.; Fan, Q.; Wang, L.; Huang, W. Cationic Conjugated Polymer/Fluoresceinamine-Hyaluronan Complex for Sensitive Fluorescence Detection of Cd44 and Tumor-Targeted Cell Imaging. *ACS Appl. Mater. Interfaces* **2014**, *6*, 19144−19153.
(50) Jiang, R.; Lu, X.; Yang, M.; Deng, W.; Fan, Q.; Huang, W. Monodispersed Brush-Like Conjugated Polyelectrolyte Nanoparticles with Efficient and Visualized Sirna Delivery for Gene Silencing. *Biomacromolecules* **2013**, *14*, 3643−3652.
(51) Feng, X.; Lv, F.; Liu, L.; Tang, H.; Xing, C.; Yang, Q.; Wang, S. Conjugated Polymer Nanoparticles for Drug Delivery and Imaging. *ACS Appl. Mater. Interfaces* **2010**, *2*, 2429−2435.
(52) Huang, Y.-Q.; Fan, Q.-L.; Lu, X.-M.; Fang, C.; Liu, S.-J.; Yu-Wen, L.-H.; Wang, L.-H.; Huang, W. Cationic, Water-Soluble, Fluorene-Containing Poly(Arylene Ethynylene)S: Effects of Water Solubility on Aggregation, Photoluminescence Efficiency, and Amplified Fluorescence Quenching in Aqueous Solutions. *J. Polym. Sci., Part A: Polym. Chem.* **2006**, *44*, 5778−5794.
(53) Choi, K. Y.; Min, K. H.; Na, J. H.; Choi, K.; Kim, K.; Park, J. H.; Kwon, I. C.; Jeong, S. Y. Self-Assembled Hyaluronic Acid Nanoparticles as a Potential Drug Carrier for Cancer Therapy: Synthesis, Characterization, and in Vivo Biodistribution. *J. Mater. Chem.* **2009**, *19*, 4102−4107.
(54) Gill, R.; Freeman, R.; Xu, J.-P.; Willner, I.; Winograd, S.; Shweky, I.; Banin, U. Probing Biocatalytic Transformations with Cdse-Zns Qds. *J. Am. Chem. Soc.* **2006**, *128*, 15376−15377.
(55) Feng, X.; Feng, F.; Yu, M.; He, F.; Xu, Q.; Tang, H.; Wang, S.; Li, Y.; Zhu, D. Synthesis of a New Water-Soluble Oligo-(Phenylenevinylene) Containing a Tyrosine Moiety for Tyrosinase Activity Detection. *Org. Lett.* **2008**, *10*, 5369−5372.
(56) Fang, S.; Hays Putnam, A. A.; LaBarre, M. J. Kinetic investigation of recombinant human hyaluronidase PH20 on hyaluronic acid. *Anal. Biochem.* **2015**, *480*, 74−81.
(57) Lakowicz, J. R. *Principles of Fluorescence Spectroscopy*, 2nd ed.; Kluwer Academic/Plenum Publishers: New York, 1999.
(58) Chong, H.; Zhu, C.; Song, J.; Feng, L.; Yang, Q.; Liu, L.; Lv, F.; Wang, S. Preparation and Optical Property of New Fluorescent Nanoparticles. *Macromol. Rapid Commun.* **2013**, *34*, 736−742.
(59) Twomey, M.; Na, Y.; Roche, Z.; Mendez, E.; Panday, N.; He, J.; Moon, J. H. Fabrication of Core-Shell Nanoparticles Via Controlled Aggregation of Semiflexible Conjugated Polymer and Hyaluronic Acid. *Macromolecules* **2013**, *46*, 6374−6378.
(60) Li, C. Poly(L-Glutamic Acid) - Anticancer Drug Conjugates. *Adv. Drug Delivery Rev.* **2002**, *54*, 695−713.

DOI: 10.1021/acsami.5b06799
ACS Appl. Mater. Interfaces 2015, 7, 21529−21537